Int. J. Heat Mass Transfer. Vol. 26, No. 4, pp. 583–595, 1983
Printed in Great Britain

0017-9310/83/040583-13 $03.00/0
Pergamon Press Ltd.

TRANSIENT BOILING HEAT TRANSFER UNDER FORCED CONVECTION

ISAO KATAOKA, AKIMI SERIZAWA† and AKIRA SAKURAI
Institute of Atomic Energy, Kyoto University, Uji, Kyoto 611, Japan

(*Received* 18 *March* 1981)

Abstract—Transient boiling heat transfer under forced convection was experimentally studied. Exponentially increasing heat input was supplied to a platinum wire in water flowing upward in a round tube at pressures from 0.143 to 1.503 MPa. In most cases, the transient boiling curve after temperature overshoot coincided with steady state boiling curve and/or its extrapolation. In these cases, the transient maximum heat flux increased with increasing velocity, subcooling and pressure, and with decreasing period and heater diameter, independently of heater length. The difference between the transient maximum heat flux and the steady state maximum heat flux was satisfactorily correlated by the exponential period.

NOMENCLATURE

a–e, exponents in equation (15);
C, constant in equation (15);
C_p, specific heat of platinum;
d, heater diameter;
d_{he}, heated equivalent diameter, $(D^2-d^2)/d$;
D, diameter of test section;
g, acceleration due to gravity;
G, mass velocity;
H_{fg}, latent heat of vaporization;
ΔH_i, enthalpy of inlet subcooling;
ΔH_{i40}, enthalpy of 40 K inlet subcooling;
K, parameter for the effect of inlet subcooling;
l, heater length;
l_0, Laplace coefficient, $\{\sigma/[g(\rho_l-\rho_v)]\}^{1/2}$;
n, exponent;
Nu, Nusselt number, $\alpha l/\lambda_l$;
Nu_B, boiling Nusselt number defined in equation (4);
Nu_{st}, steady state non-boiling Nusselt number, $\alpha_{st} l/\lambda_l$;
Nu_{tr}, transient non-boiling Nusselt number, $\alpha_{tr} l/\lambda_l$;
P, pressure;
P^*, nondimensional pressure defined in equation (4);
Pr, Prandtl number;
q, heat flux;
q_{max}, maximum heat flux;
$q_{max,0}$, maximum heat flux at zero subcooling;
$q_{max,st}$, steady state maximum heat flux;
$q_{max,st00}$, steady state maximum heat flux at zero flow and zero subcooling;
$q_{max,tr}$, transient maximum heat flux;
Q, heat generation rate per unit volume;
r, radial position;
R, radius of test section;
Re, Reynolds number, Ul/ν_l;
Re_B, boiling Reynolds number defined in equation (4);
t, time;
T, temperature;
T_m, mean temperature of heater;
T_{sat}, saturation temperature;
ΔT_{sat}, wall superheat, $T_w - T_{sat}$;
ΔT_{sub}, inlet subcooling;
T_w, wall temperature;
u, local liquid velocity;
U, mean liquid velocity.

Greek symbols

α, heat transfer coefficient;
α_{st}, steady state non-boiling heat transfer coefficient;
α_{tr}, transient non-boiling heat transfer coefficient;
ε, parameter for the effect of inlet subcooling defined in equation (8a);
λ, thermal conductivity;
ν, dynamic viscosity;
ρ, density;
σ, surface tension;
τ, exponential period of power increase;
τ_0, characteristic time.

Subscripts

l, liquid;
v, vapor;
s, solid (platinum).

Physical properties were taken at saturation temperatures unless otherwise indicated.

1. INTRODUCTION

STUDYING transient boiling heat transfer for time-dependent heat input is a fundamentally important concern in the safety evaluation of a reactivity accident in a nuclear reactor. Along with power burst experiments in nuclear reactors such as SPERT and

† Present address: Department of Nuclear Engineering, Kyoto University, Yoshida, Sakyo-ku, Kyoto 606, Japan.

BORAX, several out-of-pile experiments have been conducted to investigate the physical aspects of transient boiling heat transfer.

Several experimental works on transient boiling heat transfer have been conducted in stagnant water at atmospheric pressure with exponential power increase [1–3], step power increase [4–9], and linear power increase [10, 11]. In these experiments, quantitative knowledge of the transient non-boiling heat transfer coefficient and the transient maximum heat flux was obtained to some extent but the range of experimental conditions was limited and the data were insufficient to give physical insight into the mechanisms involved. In particular, the effects of experimental variables on transient burnout characteristics were not made clear.

At elevated pressures up to 2.1 MPa, Sakurai *et al.* [12, 13] carried out a series of transient pool boiling experiments with exponential power increase. They presented experimental correlations for transient incipient boiling superheat, transient DNB and maximum heat fluxes including the effect of pressure.

Few works have been reported on transient boiling heat transfer under forced convection. Johnson *et al.* [14, 15] conducted experiments for transient forced convective boiling with an exponential power increase over a wide range of experimental variables but the data of their experiments show considerable scatter and fail to give quantitative information about the effects of period, velocity, pressure and subcooling on the transient boiling characteristics. In Martenson's experiment [16], the flow channel was so narrow (0.18 cm gap) that bubbles generated on the heater would interact violently with the outer wall and make the phenomena more complicated. Only a few data for transient maximum heat flux are reported in his paper. Aoki *et al.* [17] studied flow and boiling characteristics under transient conditions using an annular passage with the inner tube heated exponentially with time. As in ref. [16], the annular flow passage was narrow (0.15 cm gap). The system pressure was limited to nearly atmospheric.

Thus little is known about transient boiling characteristics under forced convection. As for transient maximum heat flux, knowledge is still limited, particularly about the effects of period, velocity, pressure, subcooling and heater size, not to mention the mechanisms involved.

As is well known, various flow patterns exist in flow boiling, and the heat transfer characteristics are more or less affected by them. It is therefore necessary to study transient boiling taking these effects into consideration. In fact, a change of flow pattern along the flow direction, which is often encountered, makes transient boiling phenomena much more complicated.

Since the purpose of this paper is to clarify fundamental aspects of transient boiling under forced convection, the experimental set-up was designed in such a way that there might be no change of flow pattern and no direct interaction between the outer tube wall and vapor bubbles [18]. Under these flow conditions, effects of exponential period, velocity, subcooling, pressure and heater size were studied on transient boiling heat transfer.

2. EXPERIMENTAL APPARATUS AND PROCEDURES

Figure 1 shows a schematic diagram of the experimental apparatus used in this work. Distilled and deionized water (specific resistivity was more than 5 MΩ cm) is circulated by a pump (at a flow rate up to 300 l min^{-1}) and heated to the desired temperature level in a preheater. The flow rate is controlled by a flow-regulating valve and measured by a turbine flow meter. Water and steam are separated in a separator and expansion tank, steam being then collected in

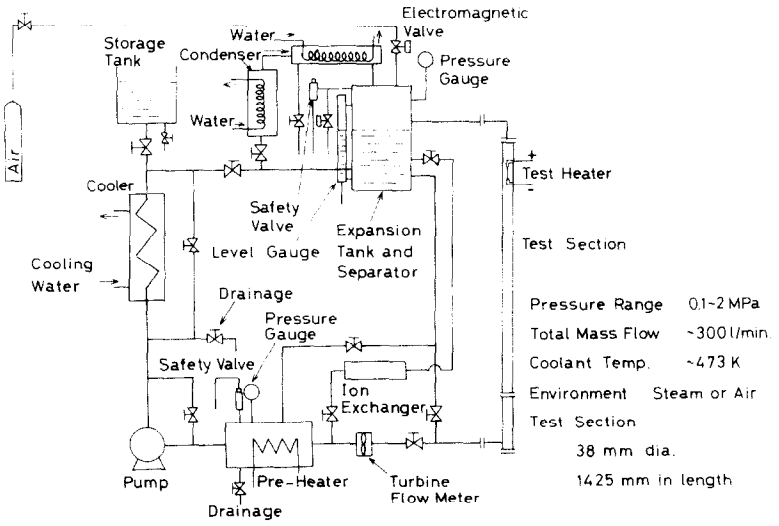

FIG. 1. Schematic diagram of the experimental apparatus.

condensers. A cooler is used to cool down circulating water to the desired temperature if necessary. The test loop is made of stainless steel with quartz glass window to allow visual observation. The test section is a round tube, 1425 mm long and 38 mm I.D. Water flows upward in this test section. The test loop is pressurized by steam in experiments at zero subcooling and by compressed air in those at subcooled conditions.

Figure 2 shows a cross-sectional view of the heated section. The heater element is a platinum wire of diameter 0.8, 1.2 and 1.5 mm and length 3.93, 7.12 and 10.04 cm. It is soldered to silver-coated copper electrodes at both ends, and located along the centerline of the flow channel at a position 1200 mm downstream from the test section inlet. The copper electrodes consist of wires and plates. The diameter of these copper wires was chosen to be 0.2–0.3 mm larger than that of the platinum wires to facilitate silver soldering between them. The copper plates of 1.5 mm in thickness, fabricated to form a streamline, were used to avoid mechanical vibrations of the heater. It was confirmed in a preliminary experiment that these electrodes did not create any series disturbance to the flow (Section 3.1.1). Potential taps (0.2 mm O.D. platinum wires) are soldered at positions about 10 mm from both ends of platinum wire heater. Mean temperature and heat flux are measured between these potential taps so as to exclude end effects of the heater.

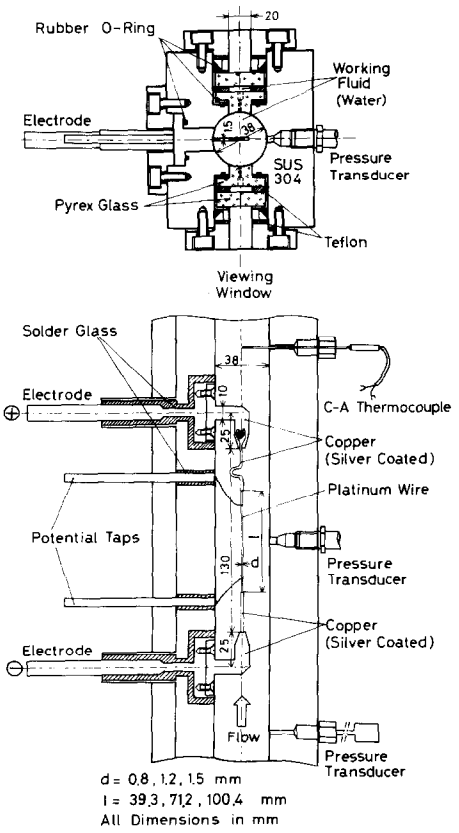

FIG. 2. Cross-sectional views of the heated section.

The details of the experimental apparatus are recorded elsewhere [18].

The power supply and data processing systems are essentially the same as those used in transient pool boiling experiments performed by Sakurai *et al.* [12, 19]. A power amplifier controlled by a high speed analog computer supplies direct current to the test heater. The analog computer computes the instantaneous power generation rate in the heater and compares it with the reference value, $Q_0 \exp(t/\tau)$. Thus the computer controls the output of the power amplifier so that the two values (heat generation rate and the reference value) are equal. In this way, exponentially increasing heat input is supplied to the heater. The analog computer also computes the instantaneous mean temperature of the heater and cuts off the power supply to the heater when the calculated mean temperature reaches a preset value. This procedure prevents the heater from actual burnout. The power amplifier consists of 800 power transistors in parallel and can supply 2000 A at 40 V. The heat generation rate in the heater is calculated from the measured voltage difference between the potential taps of the heater and the current measured using a Manganin standard resistance. The instantaneous mean temperature (volume averaged) of the heater, T_m, is calculated from the unbalanced voltage of a double bridge circuit including the heater. The instantaneous surface heat flux is then obtained from the following heat balance equation for a given heat generation rate:

$$q = \tfrac{1}{4}Qd - \tfrac{1}{4}C_p\rho_s d\frac{dT_m}{dt}. \quad (1)$$

The difference between the surface temperature and the mean temperature of the heater is not negligibly small in this experiment. Therefore, the instantaneous surface temperature of the heater, T_w, is obtained by solving the following conduction equation using a digital computer for a given heat generation rate with a given surface heat flux as a boundary condition:

$$\lambda_s \frac{1}{r}\frac{\partial}{\partial r}\left(r\frac{\partial T}{\partial r}\right) + Q = C_p\rho_s\frac{\partial T}{\partial t}. \quad (2)$$

In data processing a digital computer was used. The unbalanced voltage of the double bridge circuit including the heater, and the voltage differences between the potential taps of the heater and across the standard resistance were fed to the digital computer through a A–D converter. The fastest sampling speed of the A–D converter was 20 μs/channel.

3. RESULTS AND DISCUSSION

3.1. *Steady state performance*

Before considering transient boiling heat transfer, it is important to know the steady state boiling and non-boiling characteristics with the same heaters under the same flow conditions. Steady state experiments were therefore carried out prior to transient experiments.

The effects of velocity, subcooling, pressure and heater size on the non-boiling heat transfer coefficient, the nucleate boiling heat transfer coefficient and the maximum heat flux were studied at steady state. The results indicated that when the exponential period was larger than 5 s, the rate of heat input increase was so slow that heat transfer coefficients and maximum heat flux did not depend upon the exponential period. Therefore, experiments with exponential periods of 5–10 s can be practically regarded as steady state experiments.

3.1.1. *Non-boiling heat transfer.* As shown in Fig. 2, the heaters used in this experiment were thin platinum wires located at the center of the pipe parallel to its axis. To the present authors' knowledge, neither theoretical nor experimental results for the turbulent heat transfer coefficients of such a heat transfer configuration are available. Therefore, it is necessary to determine experimentally the non-boiling heat transfer coefficient for the heaters and flow geometry used in these experiments. At the same time, the hydrodynamic aspects around the heater must be known for the analysis of boiling phenomena. The velocity distributions just upstream of the heater were measured with a Pitot tube. Results indicated that fully-developed flows were established and velocity distributions were approximated by the one-seventh power law. Flow disturbances caused by the electrodes supporting the heater were visualized by introducing very small air bubbles into the flow as tracers. It was found that the electrodes produced no serious effects on the flow around the heater.

The experimental non-boiling heat transfer coefficient was obtained based on the mean surface temperature between the potential taps of the heater. An assumption of negligible variation of the surface temperature along the heater axis did not appear to produce erroneous results for short heaters tested in this experiment. The non-boiling heat transfer coefficient varied approximately as the 0.7 power of the velocity and increased with increasing water temperature and with decreasing heater length. The effect of heater diameter on heat transfer coefficient could not be seen over the range of the heater size of this experiment. Data for pressures in the range 0.143–1.503 MPa, liquid subcooling from 70 to 0 K (liquid temperature from 313 to 461 K), velocity from 0.39 to 4.04 m s^{-1}, heater diameter from 0.8 to 1.5 mm and heater length from 4 to 10 cm, are presented in nondimensional form in Fig. 3. Heater length was used as a characteristic length. Physical properties were taken at film temperature. Experimental data are correlated by equation (3) within $\pm 15\%$ deviations;

$$Nu = 0.2411\ Re^{0.7}\ Pr^{0.35}. \tag{3}$$

3.1.2. *Nucleate boiling heat transfer.* In the present experiment, the forced convective boiling curve in the fully-developed nucleate boiling region almost coincided with the pool boiling curve and/or its extrapolation for constant system pressure regardless

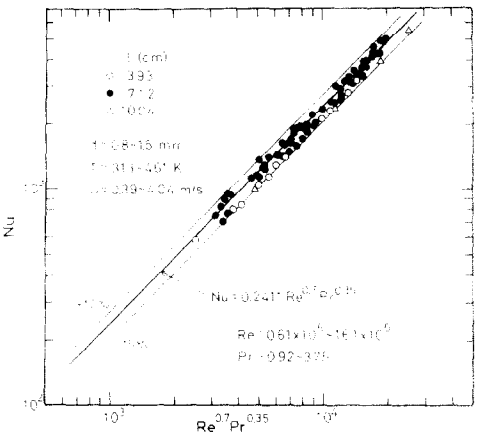

FIG. 3. Comparative representation of steady state non-boiling heat transfer coefficient.

of flow velocity and subcooling. Here the pool boiling curve is the boiling curve for inlet velocity 0 m s^{-1}. It was expressed in the form of $q \propto (\Delta T_{sat})^n$. The exponent n was about 3–4 regardless of experimental conditions.

The heat transfer coefficient increased with increasing pressure over the pressure range covered in this experiment. The heater diameter and its length had little effect on the heat transfer coefficient. Figure 4 is a representation of the experimental heat transfer coefficient in fully-developed nucleate boiling in a $Nu_B/Re_B^{0.7}$ vs $P^{*0.7}Pr^{0.35}$ diagram, where

$$Nu_B = \frac{q}{\Delta T_{sat}} \frac{\left[\dfrac{\sigma}{g(\rho_l - \rho_v)}\right]^{1/2}}{\lambda_l},$$

$$Re_B = \frac{q}{H_{fg}\rho_v} \frac{\left[\dfrac{\sigma}{g(\rho_l - \rho_v)}\right]^{1/2}}{\nu_l},$$

$$P^* = \frac{P}{[\sigma g(\rho_l - \rho_v)]^{1/2}}. \tag{4}$$

The regression is given by

$$Nu_B = 10.0 \times 10^{-4} P^{*0.7} Re_B^{0.7} Pr^{0.35}. \tag{5}$$

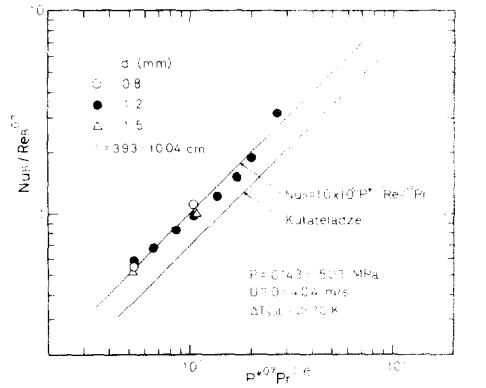

FIG. 4. Comparative representation of steady state boiling heat transfer coefficient.

The fully-developed nucleate boiling heat transfer coefficient obtained in this work was about 40% higher than Kutateladze's correlation [20].

3.1.3. *Maximum heat flux.* Figure 5 shows the effect of inlet enthalpy on the steady state maximum heat flux for the 1.2 mm O.D., 7 cm long heater at a velocity of 2.67 m s^{-1} over a pressure range of 0.143–1.503 MPa. At each pressure, the steady state maximum heat flux increases with inlet enthalpy but not always linearly. It appears that the slope in the higher subcooling range (40–70 K) is slightly steeper than that in the lower subcooling range (0–40 K). (The 40 K subcooling is indicated by the dashed line.) This tendency is noticeable at lower system pressures. A similar trend was observed for velocities other than 2.67 m s^{-1}.

Figure 6 shows the effect of velocity on the steady state maximum heat flux for the 1.2 mm O.D., 7 cm long heater at 30 K subcooling over a pressure range of 0.143–1.503 MPa. At constant pressure, the maximum heat flux increases approximately as the 0.2 power of the velocity over the velocity range 0.39–4.04 m s^{-1}. At subcooling other than 30 K, the velocity dependence of the maximum heat flux was almost the same.

As for the effect of the heater size, the maximum heat flux did not depend upon the heater length and increased only slightly with decreasing heater diameter within the limited range of heater size covered in the present work.

Recently, Katto [21, 22] correlated successfully a variety of forced convective maximum heat flux data for tubes and annuli with $l/d_{he} > 10$ by the following equations:

$$q_{max} = q_{max,0}\left(1+K\frac{\Delta H_i}{H_{fg}}\right), \tag{6}$$

$$\frac{q_{max,0}}{H_{fg}} = f\left(\frac{\rho_l}{\rho_g}\frac{\sigma\rho_l}{G^2 l}\frac{l}{d_{he}}\right). \tag{7}$$

Although l/d_{he} is very small (0.033–0.083) in the present work, a similar approach will be adopted to correlate the maximum heat flux data. However, it may not be appropriate to use the heater length as the characteristic length l in equation (7), since, in the present experiment, the maximum heat flux did not show dependence on heater length. Photographic observation revealed that the vapor masses sitting on a continuous film rise along the heater as burnout heat flux was approached. The distance between successive vapor masses was approximately constant and was the same order of magnitude as the Laplace coefficient,

$$l_0 = \left[\frac{\sigma}{g(\rho_l-\rho_v)}\right]^{1/2}.$$

Burnout might be concerned with unstable production or hydrodynamic instability of these vapor masses. As a first step, we therefore chose l_0 for l in correlating the experimental results. The value of K in equation (6) was determined by least squares fitting, using experimental data over a subcooling range of 0–70 K. The result is given by

$$K = 0.03648\left(\frac{l_0}{d_{he}}\right)^{-0.20}\left(\frac{\rho_v}{\rho_l}\right)^{-0.79}+\varepsilon \tag{8a}$$

where

$$\varepsilon = 0 \quad (\Delta T_{sub} = 0\text{–}40\ \text{K}),$$

$$= 0.00808\left(\frac{\rho_v}{\rho_l}\right)^{-1.09}\frac{\Delta H_i - \Delta H_{i40}}{\Delta H_i} \quad (\Delta T_{sub} = 40\text{–}70\ \text{K}). \tag{8b}$$

In this experiment, d_{he} ranged from 1805 to 963 mm for heater diameters from 0.8 to 1.5 mm.

On the other hand, $q_{max,0}$ in equation (6) was determined by extrapolating the experimental value of q_{max} to the zero subcooling condition. The $q_{max,0}$ obtained is satisfactorily correlated by equation (9),

$$\frac{q_{max,0}}{GH_{fg}} = 0.3740\left(\frac{\rho_v}{\rho_l}\right)^{0.66}\left(\frac{\sigma\rho_l}{G^2 l_0}\right)^{0.40}. \tag{9}$$

By substituting equations (8) and (9) into equation (6),

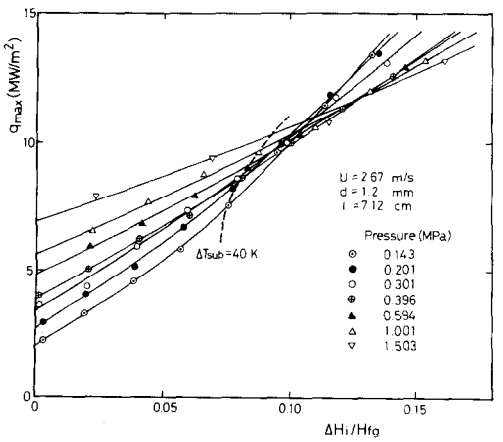

FIG. 5. The variation of steady state maximum heat flux with inlet enthalpy and pressure.

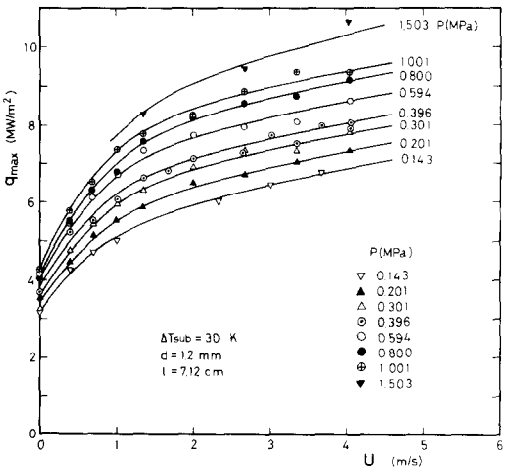

FIG. 6. The variation of steady state maximum heat flux with velocity and pressure.

we have

$$\frac{q_{max}}{GH_{fg}} = 0.3740\left(\frac{\rho_v}{\rho_l}\right)^{0.66}\left(\frac{\sigma\rho_l}{G^2 l_0}\right)^{0.40} \times\left\{1+\left[0.03648\left(\frac{l_0}{d_{he}}\right)^{-0.20}\left(\frac{\rho_v}{\rho_l}\right)^{0.79}+\varepsilon\right]\frac{\Delta H_i}{H_{fg}}\right\} \quad (10)$$

where ε is given by equation (8b) and is a small contribution (15% at most). It should be noted in equation (10) that q_{max} varies as the 0.2 power of the mass velocity G. This dependence on the mass velocity appears to be weak compared with those reported elsewhere. A comparison of equation (10) with the present steady state maximum heat flux data is made in Fig. 7 in a

$$\frac{q_{max}}{GH_{fg}} \quad \text{vs} \quad \left(\frac{\rho_v}{\rho_l}\right)^{0.66}\left(\frac{\sigma\rho_l}{G^2 l_0}\right)^{0.40}\left(1+K\frac{\Delta H_i}{H_{fg}}\right)$$

diagram. The data scatter around equation (10) within $\pm 10\%$ error bands.

Borishansky *et al.* [23] reported steady state maximum heat flux under forced convection in an annular passage whose geometry is similar to that in our experiment. In their experiment, a 3 mm O.D., 7.2 cm long heater is located in a 19 mm I.D. tube with water and ethyl alcohol flowing at velocities up to 2.5 m s^{-1} at atmospheric pressure ($l/d_{he} = 0.61$). Figure 8 shows a comparison of the present correlation, equation (10), with their data. Except for the case of water with 46.6 K subcooling, equation (10) satisfactorily agrees with their data.

Equation (10) is originally derived for the experimental data at velocity higher than 0.39 m s^{-1} and, therefore, it may not be applied to those at lower velocity or stagnant condition. Measurements of the steady state maximum heat flux at zero flow were made by closing the flow regulating valve. The experimental data of the steady state maximum heat flux at zero flow and zero subcooling (hereafter called $q_{max,st00}$) were

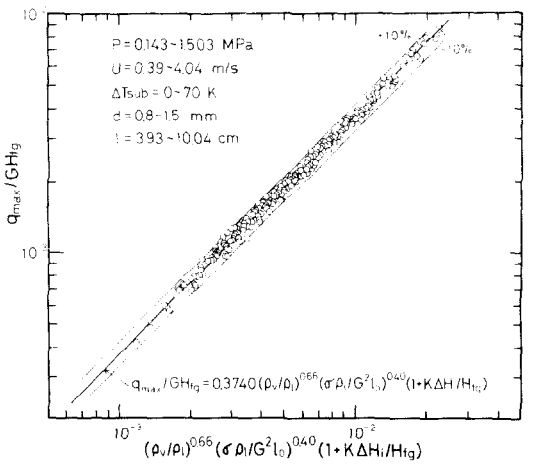

FIG. 7. Comparative representation of steady state maximum heat flux.

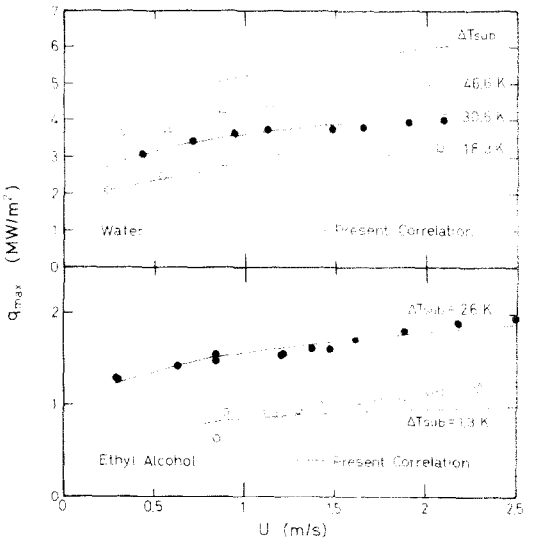

FIG. 8. Comparison of equation (10) with the experimental data of Borishansky *et al.*

compared with the Kutateladze's correlation for maximum heat flux in saturated pool boiling [20], which is given by

$$\frac{q_{max,st00}}{H_{fg}\rho_v} = 0.16\left[\frac{\sigma g(\rho_l-\rho_v)}{\rho_v^2}\right]^{1/4}. \quad (11)$$

Agreement was quite good between Kutateladze's correlation and the present data.

Under forced convection, there are several different burnout mechanisms suggested for different flow patterns [24]. Under the particular flow condition of this experiment and Borishansky *et al.*'s (small heater diameters, short heater lengths), quality change along the heater is small and burnout quality is low. Therefore, it is likely that steady burnout is caused not by dryout of liquid film flow but by bubble coalescence and vapor blanketing near the heater surface.

3.2. *Transient state performance*

3.2.1. *Transient non-boiling heat transfer.* During a period from the initiation of heating to the boiling inception, heat is transferred to water by transient non-boiling heat transfer. Analytical or experimental works have been presented by Chambré *et al.* [25] and Soliman *et al.* [26] for transient non-boiling heat transfer under forced convection with exponential heat input to flat plates. Chambré *et al.* assumed a slug flow model where the velocity profile is uniform, while Soliman *et al.* took into consideration the turbulent boundary layer over a flat plate and compared the result with experiments. Both analyses predicted that the transient non-boiling heat transfer coefficient has initially a decreasing tendency with time, t, and attained an asymptotic value for $t/\tau \geqslant l/\tau U$ where t is the time elasped from the initiation of heating.

The present experiment showed a trend similar to those predicted by the above analyses. That is, the

transient non-boiling heat transfer coefficient had asymptotic values for $t/\tau \geqslant 3$. Particular attention should be paid to these asymptotic values of the heat transfer coefficient. (Therefore the heat transfer coefficient means hereafter its asymptotic value in this section.) The present experiment also showed that the heat transfer coefficient increased with decreasing period, and increased with an increase in velocity and heater length for constant period. However, the heater diameter had little effect on the transient non-boiling heat transfer coefficient within the limited range of heater diameters tested in the present work (0.8–1.5 mm O.D.).

Figure 9 represents the experimental data in Nu_{tr}/Nu_{st} vs $\tau U/l$ diagram, where Nu_{tr} is the Nusselt number associated with the transient non-boiling heat transfer coefficient and Nu_{st} is associated with the steady state coefficient (see Nomenclature). The data are correlated by equation (12) within $\pm 20\%$ deviation,

$$\frac{Nu_{tr}}{Nu_{st}} = 1 + 0.1448\left(\frac{\tau U}{l}\right)^{-0.97}. \tag{12}$$

As stated earlier, the flow around the heater is fully turbulent. Hence, a turbulent boundary layer treatment should be applied to analyze the non-boiling heat transfer characteristics. But the structure of turbulent boundary layer around such thin wires as those used in the present experiment has not been yet made clear. We will therefore adopt a slug flow model as a first approximation to analyze the effect of power transient on non-boiling heat transfer around a cylindrical wire. Here, slug flow is flow with uniform velocity distribution around the heater. We assume the physical properties of the fluid are constant and conduction effects in the flow direction are negligible. Then the solution is given by equation (13) for $t/\tau \geqslant l/\tau U$ for exponential heat input with negligible heat capacity of the heater. Nu_{tr} is correlated in terms of $l/\tau U$, l/d, Reynolds number, and Prandtl number by

$$\frac{Nu_{tr}}{Nu_{st}} = \frac{\left(\frac{4}{3\sqrt{\pi}}\right)(1-\xi)\left(\frac{l}{\tau U}\right)^{1/2}}{\left(1-\frac{1}{2}\frac{\tau U}{l}\right)\operatorname{erf}\left(\frac{l}{\tau U}\right)^{1/2} + \left(\frac{\tau U}{\pi l}\right)^{1/2}\exp\left(-\frac{l}{\tau U}\right) - \frac{8}{3}\xi\left(\frac{\tau U}{\pi l}\right)^{1/2}\left[1-\frac{\tau U}{l}+\frac{\tau U}{l}\exp\left(-\frac{l}{\tau U}\right)\right]} \tag{13a}$$

where

$$\xi = \frac{3}{8}(\pi)^{1/2}\left(\frac{l}{d}\right)\left[\frac{1}{(RePr)^{1/2}}\right]. \tag{13b}$$

Here, Nu_{st} is derived theoretically and is given by

$$Nu_{st} = \frac{3}{4}(\pi)^{1/2}\left(\frac{1}{1-\xi}\right)(RePr)^{1/2}. \tag{14}$$

Equations (13) and (14) are derived in the same manner as Chambré's treatment; by consulting the textbook by Carslaw and Jaeger [27]. Equation (13a) reduces to Chambré's equation for a flat plate with $\xi = 0$. The present analysis, equation (13), is also compared in Fig. 9 with our own data. Under the experimental conditions of present work, ξ ranged from 0.021 to 0.079. In this range of ξ, ξ had little effect on Nu_{tr}/Nu_{st} in equation (13a). (Therefore, in Fig. 9, the curve for $\xi = 0.079$ indicates representative of the present experiment.)

It is noted in Fig. 9 that equation (13a) predicts well the experimental trends, though the model cannot reflect quantitatively the experimental tendencies in Nu_{tr} and Nu_{st} [compare, for example, equation (14) with equation (3)]. More strict models are needed to take into account the effects of heat capacity and flow structure such as the turbulence and the velocity field around a thin wire.

3.2.2. *Transient boiling heat transfer.* Figure 10(a) shows steady and transient boiling curves for the 1.2 mm O.D., 7 cm long heater at pressure 0.396 MPa, subcooling 10 K and velocity 1.35 m s^{-1}. The exponential period of power increase ranges from 10 s (steady state) to 5 ms. For each period, the transient boiling curve shifts towards higher wall superheat than the steady state boiling curve [the solid curve in Fig. 10(a)] for a certain time after commencement of boiling. At higher heat flux, the transient boiling curve coincides with the steady state boiling curve and/or its extrapolation. This type of transient boiling is called 'A-type' transient boiling in this paper. Most of the transient boiling achieved in the present work was A-type. Figure 10(b) shows similar curves for a heater of different size (0.8 mm O.D.) at pressure 0.396 MPa, subcooling 30 K and velocity 1.35 m s^{-1}. The results indicated that the transient boiling curve is A-type for the period larger than 20 ms but for the period smaller than 14 ms the curves did not coincide with the steady state boiling curve and/or its extrapolation. On these boiling curves the wall superheat remains higher than that on steady state boiling curve and/or its extrapolation until the maximum heat flux is reached. This type of transient boiling curve is called 'B-type' here.

B-type boiling was observed in the following conditions: For 0.8 mm O.D., 7 cm long heater: pressure lower than 0.396 MPa, subcooling lower than 30 K and period smaller than 14 ms. For 1.2 mm O.D., 7 cm long heater: pressure lower than 0.143 MPa, subcooling lower than 10 K and period smaller than 30 ms. For 1.5 mm O.D., 7 cm long heater it was not observed. For 1.2 mm O.D., 10 cm long heater it was observed for pressures lower than 0.396 MPa, subcooling lower than 30 K and periods smaller

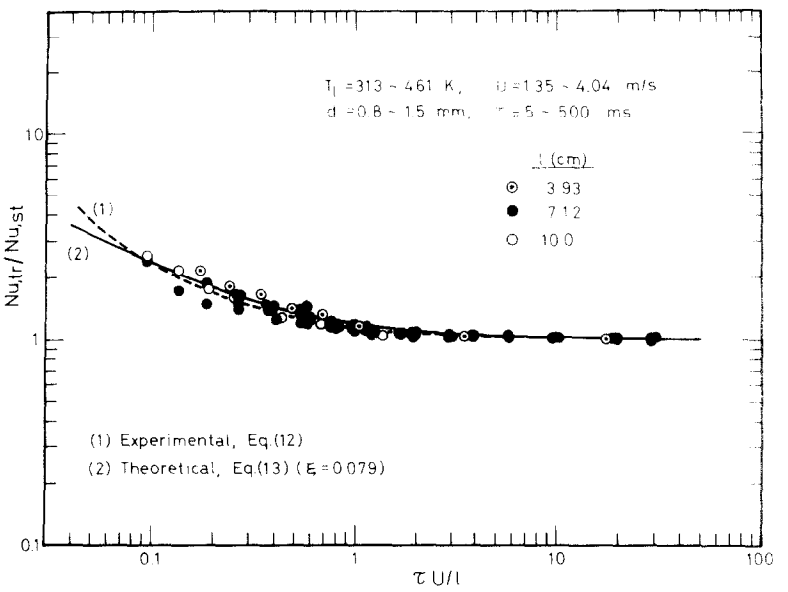

FIG. 9. Comparative representation of transient non-boiling heat transfer coefficient.

than 14 ms. For 1.2 mm O.D., 4 cm long heater: not observed.

B-type boiling is also interesting and important in its mechanisms and from engineering points of view. However, B-type boiling was observed under limited conditions and A-type boiling was mostly observed in the present work. Therefore, our concern is directed to A-type boiling. To clarify B-type boiling in more detail is beyond the scope of this work.

As mentioned above, the transient boiling curve had a portion where the wall superheat shifts to the right of the steady state boiling curve. A similar phenomenon is reported to have been observed in pool boiling of water [13].

3.2.3. *Transient maximum heat flux.* Figure 11(a) shows the effects of the exponential period on the transient maximum heat flux for 0.8 mm O.D., 7 cm long heater at pressure 0.396 MPa, subcooling 30 K and velocity from 1.35 to 4.04 m s^{-1}. In this figure, the RHS of the dot-dash line is a region of A-type transient boiling and the LHS a region of B-type. In the A-type region, the transient maximum heat flux increases with decreasing period at constant velocity, whereas, in the B-type region, the transient maximum heat flux decreases with the period and then increases. As stated in the previous section, the boiling curves encountered in the present experiment were mostly A-type, and B-type boiling was exceptional. A-type transient

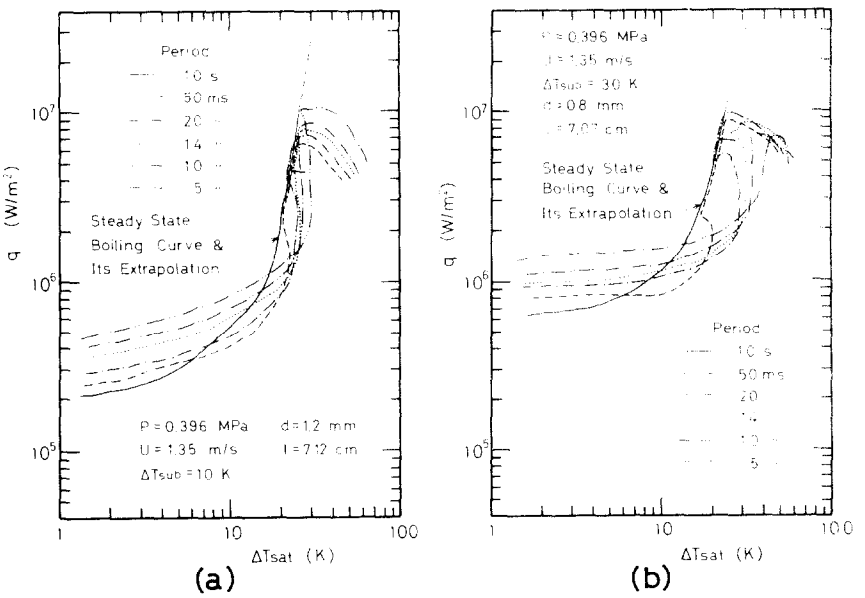

FIG. 10. Transient boiling curves for (a) $d = 1.2$ mm and $\Delta T_{sub} = 10$ K and (b) $d = 0.8$ mm and $\Delta T_{sub} = 30$ K.

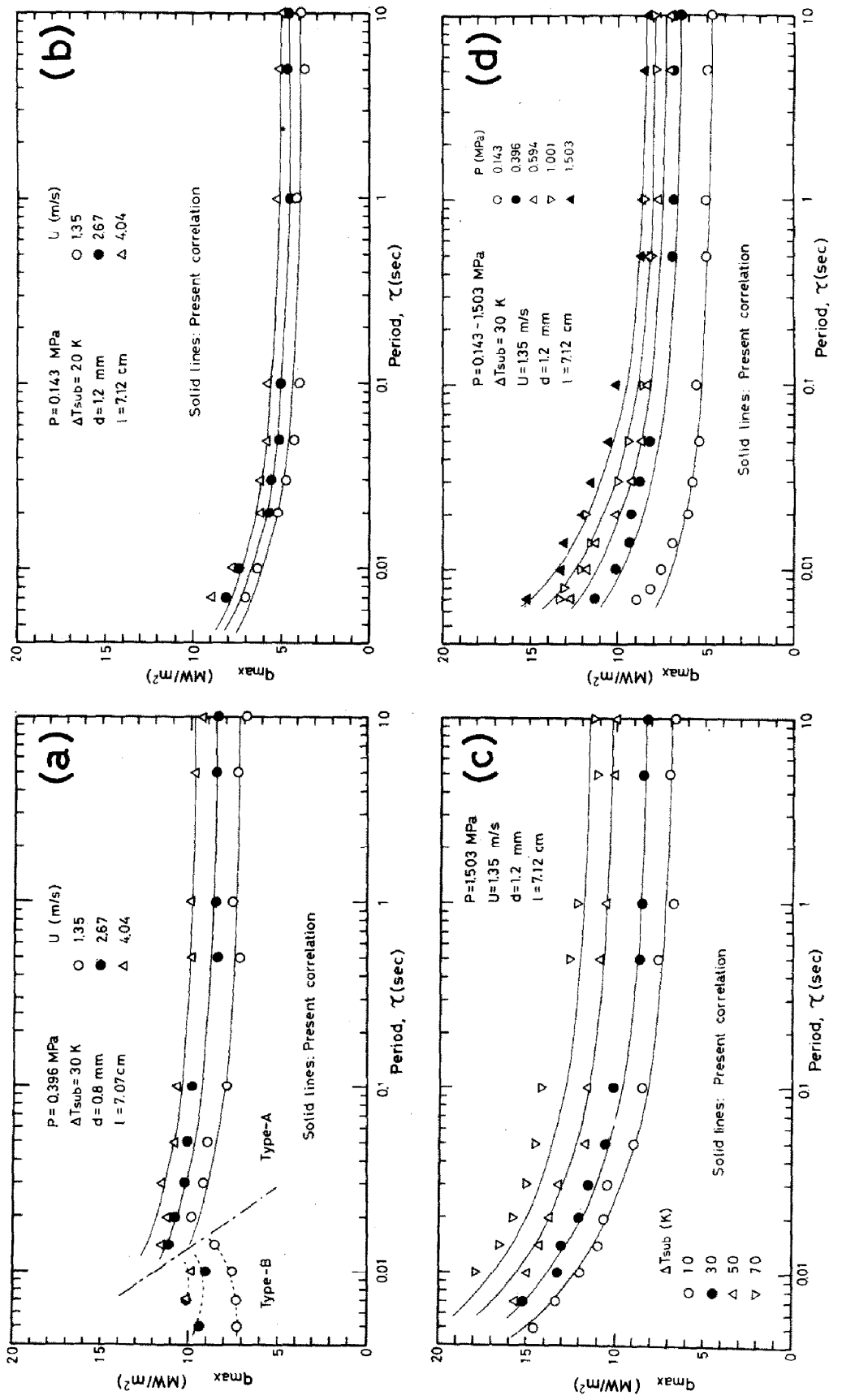

FIG. 11. The variation of transient maximum heat flux with period and (a) velocity ($d = 0.8$ mm), (b) velocity ($d = 1.2$ mm), (c) subcooling ($d = 1.2$ mm) and (d) pressure ($d = 1.2$ mm).

maximum heat flux will be discussed below in more detail.

The transient maximum heat flux for the 1.2 mm O.D., 7 cm long heater is plotted against the period in Figs. 11(b), (c) and (d). Solid curves in Figs. 11(a), (b), (c) and (d) represent equation (17) and will be discussed later. Figure 11(b) shows the effect of velocity, Fig. 11(c) the effects of subcooling and Fig. 11(d) the effect of pressure. The transient maximum heat flux increases as the period is decreased. Similarly to the steady state maximum heat flux, the transient maximum heat flux increases with increasing velocity, subcooling and pressure for a constant period. Over the heater length range of 4–10 cm, the transient maximum heat flux was independent of the heater length. As for the effect of heater diameter, the transient maximum heat flux increased with decreasing heater diameter for a constant period. From this experimental evidence, it seems practical to use the difference between the transient maximum heat flux and the steady state maximum heat flux in correlating the transient maximum heat flux.

In fact, the difference between the transient maximum heat flux and steady state flux varied approximately as the -0.6 power of the period over the pressure, velocity, subcooling and heater sizes ranges of this experiment. Taking this into account, the following dimensional analysis will be adopted.

As stated in Section 3.1.3, the steady state maximum heat flux is expressed in the form of five nondimensional groups,

$$\frac{q}{GH_{fg}}, \frac{\rho_v}{\rho_l}, \frac{\sigma\rho_l}{G^2 l_0}, \frac{l_0}{d_{he}} \quad \text{and} \quad \frac{\Delta H_i}{H_{fg}}.$$

By applying dimensional analysis to the case of transient maximum heat flux, we obtain another nondimensional group, $\tau_0 G/\rho_l l_0$ in addition to the above five, where τ_0 is a characteristic time specifying the transient maximum heat flux. In the present work, we chose the exponential period, τ, of the power increase as the characteristic time, τ_0. We further assume the following nondimensional expression for the transient maximum heat flux because the transient maximum heat flux approaches the steady state maximum heat flux when the exponential period tends to infinity:

$$\frac{q_{max,tr}-q_{max,st}}{GH_{fg}} = C\left(\frac{\rho_v}{\rho_l}\right)^a \left(\frac{\sigma\rho_l}{G^2 l_0}\right)^b \times \left(\frac{l_0}{d_{he}}\right)^c \left(\frac{\Delta H_i}{H_{fg}}\right)^d \left(\frac{\tau G}{\rho_l l_0}\right)^e. \quad (15)$$

The experimental data for A-type boiling were used to determine a–e in equation (15). This showed that $(q_{max,tr}-q_{max,st})$ had little dependence on (l_0/d_{he}) and $(\Delta H_i/H_{fg})$, i.e. c and d are zero. a, b and e have been determined by least squares fitting, giving

$$\frac{q_{max,tr}-q_{max,st}}{GH_{fg}} = 0.2038\left(\frac{\rho_v}{\rho_l}\right)^{0.52} \times \left(\frac{\sigma\rho_l}{G^2 l_0}\right)^{0.19} \left(\frac{\tau G}{\rho_l l_0}\right)^{-0.63}. \quad (16)$$

Figure 12 shows plots of the transient maximum heat flux in terms of

$$\left(\frac{q_{max,tr}-q_{max,st}}{GH_{fg}}\right)\left(\frac{\rho_v}{\rho_l}\right)^{-0.52}\left(\frac{\sigma\rho_l}{G^2 l_0}\right)^{-0.19} \text{ vs } \left(\frac{\tau G}{\rho_l l_0}\right)$$

for subcooling from 0 to 40 K, velocity from 1.35 to 4.04 m s^{-1}, pressure from 0.143 to 1.503 MPa, heater

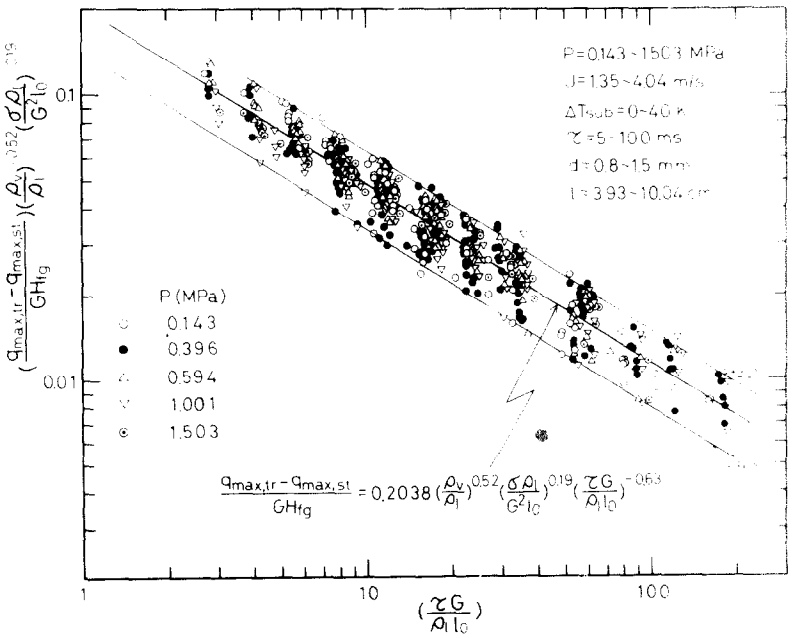

FIG. 12. Comparative representation of transient maximum heat flux.

diameter from 0.8 to 1.5 mm and heater length from 3.93 to 10.04 cm and for A-type boiling. The data lie within $\pm 30\%$ of equation (16).

By substituting equation (10) into equation (16), we finally obtain equation (17) for the transient maximum heat flux,

$$\frac{q_{max,tr}}{GH_{fg}} = 0.3740\left(\frac{\rho_v}{\rho_l}\right)^{0.66}\left(\frac{\sigma\rho_l}{G^2 l_0}\right)^{0.40} \times\left\{1+\left[0.03648\left(\frac{l_0}{d_{he}}\right)^{-0.20} \times\left(\frac{\rho_v}{\rho_l}\right)^{-0.79}+\varepsilon\right]\frac{\Delta H_i}{H_{fg}}\right\}+0.2038\left(\frac{\rho_v}{\rho_l}\right)^{0.52} \times\left(\frac{\sigma\rho_l}{G^2 l_0}\right)^{0.19}\left(\frac{\tau G}{\rho_l l_0}\right)^{-0.63} \quad (17)$$

where ε is given by equation (8b),

$$\varepsilon = 0 \quad (\Delta T_{sub} = 0\text{–}40\ \text{K})$$

$$= 0.00808\left(\frac{\rho_v}{\rho_l}\right)^{-1.09}\frac{\Delta H_i - \Delta H_{i40}}{\Delta H_i} \quad (\Delta T_{sub} = 40\text{–}70\ \text{K}). \quad (8b)$$

Figure 13 shows a comparison of equation (17) with the experimental data. Over the experimental range of this work, the measured maximum heat flux for A-type boiling lies within $\pm 20\%$ of that calculated.

Equation (16) can be rewritten as

$$\frac{q_{max,tr}-q_{max,st}}{q_{max,st00}} = 1.274\left(\frac{\rho_v}{\rho_l}\right)^{-0.30}\left\{\frac{\tau[\sigma g(\rho_l-\rho_v)/\rho_v^2]^{1/4}}{l_0}\right\}^{-0.63} \quad (18)$$

where $q_{max,st00}$ is given by equation (11). For water at pressures from 0.1 to 5 MPa, equation (18) can be approximated for practical uses by

$$\frac{q_{max,tr}-q_{max,st}}{q_{max,st00}} = 0.083\,\tau^{-0.63} \quad (19)$$

where τ is in s. Equation (19) correlates the present data as accurately as equation (16).

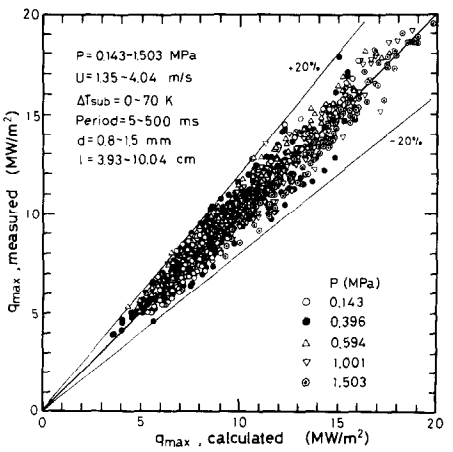

FIG. 13. Comparison of equation (15) with the measured transient maximum heat flux.

As stated in Section 3.1.3, under the flow conditions of this experiment, it is considered that burnout is caused by bubble coalescence and vapor blanketing. Even at steady state maximum heat flux, the transition to film boiling, and the resulting heater overheat, occurs over a certain (though very short) time period. This is partly because the heater possesses finite heat capacity, and partly because it takes time for hydrodynamic instability to grow and for the liquid layer under the vapor blanket to vaporize.

In the case of the transient power increase, a similar process is assumed to occur for A-type boiling, where the transient boiling curve coincides with the steady state boiling curve and/or its extrapolation. Under such circumstances, after the heat flux reaches the steady state maximum heat flux, it will continue to increase for a time duration needed for the growth of hydrodynamic instability and the evaporation of liquid layer under vapor blanket.

The present study gives quantitative information about forced convective transient boiling heat transfer with fine wires. However, much remains to be studied. The mechanisms of forced convective transient boiling phenomena need to be clarified based on more detailed observations of flow characteristics and bubble behavior under transient conditions.

4. CONCLUSIONS

Forced convective transient boiling heat transfer for exponential heat input using platinum wire heaters was studied. The following conclusions are drawn:

(1) The steady state non-boiling heat transfer coefficient is correlated within $\pm 15\%$ by equation (3), where the heater length, l, appears as a characteristic length instead of diameter.

(2) The steady state heat transfer coefficient in fully-developed nucleate boiling region was 40% higher than Kutateladze's prediction.

(3) The steady state maximum heat flux increased with increasing velocity, pressure and subcooling and with decreasing heater diameter within the range of parameters covered in the present experiment. The steady state maximum heat flux is correlated by equation (10) within $\pm 10\%$. Equation (10) agrees well with Borishansky *et al.*'s data for water and ethyl alcohol.

(4) The transient non-boiling heat transfer coefficient increased with decreasing period and increased with an increase in velocity and heater length for constant period. The transient non-boiling heat transfer coefficient is correlated by equation (12) within $\pm 20\%$. Equation (13), an analytical correlation obtained based on a slug flow model, predicts the experimental trends.

(5) Two types of transient boiling were observed. In A-type boiling, the transient boiling curve coincided at higher heat flux with the steady state boiling curve and/or its extrapolation. In B-type boiling, the wall superheat remained higher than that on the steady state boiling curve and/or its extrapolation until the maximum heat flux was reached. Under most of the experimental conditions tested, A-type boiling was observed.

(6) In A-type boiling, the transient maximum heat flux increased with decreasing period and with increasing pressure, velocity and subcooling. The difference between the transient maximum heat flux and the steady state flux varied approximately as the -0.6 power of the period over the pressure, velocity, subcooling and heater-size ranges of this experiment.

(7) The nondimensional correlation for the transient maximum heat flux, equation (17), is presented for A-type boiling. Equation (17) correlates experimental data within $\pm 20\%$. For water at pressures from 0.1 to 5 MPa, equation (15) can be approximated by equation (18).

Acknowledgements – The authors gratefully acknowledge the financial support by the Ministry of Education and the Toray Science Foundation. Thanks are also expressed to Dr M. Shiotsu and Mr K. Hata for their assistance in part of this experiment.

REFERENCES

1. M. W. Rosenthal, An experimental study of transient boiling, *Nucl. Sci. Engng* **2**, 640–656 (1957); M. W. Rosenthal and R. L. Miller, ORNL-2294 (1957).
2. W. B. Hall and W. C. Harrison, Transient boiling of water at atmospheric pressure, *Proc. 3rd Int. Heat Transfer Conf.* Chicago (1966).
3. A. Sakurai, K. Mizukami and M. Shiotsu, Experimental studies on transient boiling heat transfer and burnout, *Proc. 4th Int. Heat Transfer Conf.*, Paris (1970).
4. R. Cole, Investigation of transient pool boiling due to sudden large power surge, NACA Technical Note 3885 (1956).
5. S. Hayashi, T. Iwazumi, J. Wakabayashi, A. Sakurai, H. Aoki and M. Kitamura, Experimental study of the temperature overshoot and the delay time of the transient boiling, *J. Atomic Energy Soc. Japan* **2**, 736–741 (1960) (in Japanese).
6. S. Hayashi, A. Sakurai and T. Iwazumi, Transient heat transfer in heterogeneous water reactor (I), *J. Atomic Energy Soc. Japan* **5**, 403–411 (1963) (in Japanese).
7. H. Lurie and H. A. Johnson, Transient pool boiling of water on vertical surface with a step in heat generation, *J. Heat Transfer* **84**, 217–224 (1962).
8. T. Sato, I. Michiyoshi, K. Takeuchi and K. Kondo, Experimental studies of the burnout under the boiling (I), *Trans. JSME* **27**, 722–730 (1961) (in Japanese).
9. T. Sato, I. Michiyoshi and K. Takeuchi, Studies of the burnout under the boiling (II), *Trans. JSME* **27**, 1817–1822 (1961) (in Japanese).
10. F. Tachibana, M. Akiyama and H. Kawamura, Heat transfer and critical heat flux in transient boiling (I), *J. Nucl. Sci. Technol.* **5**, 117–126 (1968).
11. H. Kawamura, F. Tachibana and M. Akiyama, Heat transfer and DNB heat flux in transient boiling, *Proc. 4th Int. Heat Transfer Conf.*, Paris (1970).
12. A. Sakurai and M. Shiotsu, Transient pool boiling heat transfer (I), *J. Heat Transfer* **99**, 547–553 (1977).
13. A. Sakurai and M. Shiotsu, Transient pool boiling heat transfer (II), *J. Heat Transfer* **99**, 554–560 (1977).
14. H. A. Johnson, V. E. Shrock *et al.*, Reactor heat transients project, University of California, Berkeley, USAEC, TID 4500 Reports: SAN 1001 (1961) to SAN 1013 (1966).
15. H. A. Johnson, Transient boiling heat transfer to water, *Int. J. Heat Mass Transfer* **14**, 67–82 (1971).
16. A. J. Martenson, Transient boiling in small rectangular channels, WAPD-T-1290 (1963).
17. S. Aoki, Y. Kozawa and H. Iwasaki, Boiling and burnout phenomena under transient heat input, *Trans. JSME* **41**, 2950–2959 (1975) (in Japanese).
18. A. Serizawa and A. Sakurai, unpublished work (1973).
19. A. Sakurai, M. Shiotsu and K. Hata, Transient boiling caused by rapid depressurization from initial nonboiling state, in *Multiphase Transport: Fundamental, Reactor Safety, Applications* (edited by T. N. Veziroglu) Vol. 2, pp. 724–747. Hemisphere, Washington (1980).
20. S. S. Kutateladze, *Heat Transfer in Condensation and Boiling*, AEC-tr-3770 (1959).
21. Y. Katto, A generalized correlation of critical heat flux for the forced convection boiling in vertical uniformly heated round tubes, *Int. J. Heat Mass Transfer* **21**, 1527–1542 (1978).
22. Y. Katto, Generalized correlations of critical heat flux for uniformly heated annuli, *Int. J. Heat Mass Transfer* **22**, 575–584 (1979).
23. V. M. Borishansky and B. S. Fokin, Onset of heat transfer crisis with unsteady increase in heat flux, *Heat Transfer Soviet Res.* **1**, 27–55 (1969).
24. L. S. Tong and G. F. Hewitt, Overall viewpoint of flow boiling CHF mechanism, ASME Paper 72-HT-54 (1972).
25. H. A. Johnson and P. L. Chambré, Slug conduction solution for exponential heat generation in a thin flat plate, USAEC Report SAN-1009 (1963) [quoted from USAEC Report SAN-1013 (1963)].
26. M. Soliman and H. A. Johnson, Transient heat transfer for forced convection flow over a flat plate of appreciable thermal capacity and containing an exponential time-dependent heat source, *Int. J. Heat Mass Transfer* **11**, 27–38 (1968).
27. H. S. Carslaw and J. C. Jaeger, *Conduction of Heat in Solids*, Oxford University Press, Oxford (1959).

TRANSFERT THERMIQUE PAR EBULLITION VARIABLE EN CONVECTION FORCEE

Résumé – On étudie expérimentalement le transfert thermique par ébullition variable en convection forcée. Un flux de chaleur croissant exponentiellement est fourni à un fil de platine dans l'eau s'écoulant de façon ascendante dans un tube, à des pressions variant entre 0,143 et 1,503 MPa.

Dans la plupart des cas, la courbe de l'ébullition transitoire coincide avec celle du régime permanent ou son extrapolation. Dans ces cas, le flux de chaleur transitoire maximal croît quand croissent la vitesse, le sous-refroidissement et le pression, et quand diminuent la période et le diamètre du chauffoir, indépendamment de la longueur du chauffoir. La différence entre le flux maximal transitoire et celui permanent est correctement exprimée par la période exponentielle.

INSTATIONÄRE WÄRMEÜBERTRAGUNG BEIM SIEDEN UNTER DEN BEDINGUNGEN ERZWUNGENER KONVEKTION

Zusammenfassung—Die instationäre Wärmeübertragung beim Sieden unter den Bedingungen erzwungener Konvektion wurde experimentell untersucht. Die Wärmezufuhr an das Wasser, das bei Drücken von 0,143 bis 1,503 MPa in einem Kreisrohr aufwärts strömt, erfolgt durch einen Platindraht, der exponentiell ansteigend erwärmt wird. In dem meisten Fällen stimmte die instationäre Siedekurve nach dem Überschwingen der Temperatur mit der stationären Siedekurve und/oder ihrer Extrapolation überein. In diesen Fällen stieg der instationäre Wärmestrom mit der Zunahme von Geschwindigkeit, Unterkühlung und Druck sowie mit der Abnahme von Periodendauer und Hitzdrahtdurchmesser an, unabhängig von der Hitzdrahtlänge. Der Unterschied zwischen dem instationären und dem stationären maximalen Wärmestrom konnte befriedigend mit der Periodendauer der exponentiell ansteigenden Wärmezufuhr korreliert werden.

ТЕПЛОПЕРЕНОС В ПЕРЕХОДНОМ РЕЖИМЕ КИПЕНИЯ ПРИ ВЫНУЖДЕННОЙ КОНВЕКЦИИ

Аннотация—Проведено экспериментальное исследование теплопереноса в переходном режиме кипения при вынужденной конвекции. Экспоненциально возрастающая тепловая нагрузка подавалась на платиновую проволоку, помещенную в круглую трубу с восходящим потоком воды, при этом давление изменялось от 0,143 до 1,503 Мн/м^2. В большинстве случаев кривая переходного режима кипения после достижения максимального значения температуры совпадала с кривой стационарного режима кипения и(или) ее экстраполяцией. При этом величина переходного максимального теплового потока возрастала с увеличением скорости, недогрева и давления и с уменьшением продолжительности подвода тепла и диаметра нагревателя независимо от его длины. Разность между величинами максимальных тепловых потоков в переходном и стационарном режимах кипения удовлетворительно описывается с помощью экспоненциальной зависимости.